Protoplasma (1994) 178: 66–80

PROTOPLASMA

© Springer-Verlag 1994
Printed in Austria

Structure and development of the dolipore septum in *Pisolithus tinctorius*

D. A. Orlovich* and **Anne E. Ashford**

School of Biological Science, The University of New South Wales, Kensington, New South Wales

Received April 27, 1993
Accepted November 11, 1993

Summary. The structure and development of dolipore septa and associated clamp connections are described for the ectomycorrhizal holobasidiomycete *Pisolithus tinctorius*, following freeze-substitution of growing hyphae. Septa in the main hypha and clamp are formed synchronously and are completed within a few minutes. They are produced by a furrowing of the plasma membrane and concurrent wall deposition. Fine filaments occur in a ring adjacent to the deposited septum. Radial and parallel filaments, that occur in a complex arrangement around the apex of the membrane infolding, are likely to be instrumental in bringing about cytokinesis. The pore opening is reduced to about 140 nm and there is still no parenthesome capping it, indicating that this is organised late in septal pore development. At maturity, the pore is surrounded by a dome-shaped, perforate parenthesome on each side and is filled with filamentous electron-opaque material which spreads laterally over the adjacent septal membrane. Filaments radiate from this material to contact the parenthesome. The entire structure is interpreted as a co-ordinated whole, with the radiating filaments anchoring and supporting the parenthesome, so that its shape, position and orientation in relation to the pore entrance are maintained. Similarly the rough endoplasmic reticulum (ER) parallel to the septum also appears anchored to the plasma membrane by short fine filaments. Continuities between the lumen of this ER and the parenthesome could not be found, and the evidence indicates that the rim of the parenthesome is anchored to the plasma membrane rather than to the ER. Septal structure and development are discussed in relation to symplastic continuity in the hyphae and cell-to-cell transport across the dolipore.

Keywords: Ectomycorrhizal fungus; Freeze-substitution; *Pisolithus tinctorius*; Dolipore septum; Parenthesome; Symplastic transport.

Abbreviation: ER endoplasmic reticulum

Introduction

The dolipore septum with its associated clamp connection is thought to be part of a complex mechanism evolved in dikaryotic mycelia of many basidiomycetes ensuring an ordered migration of nuclei so that new cells each receive a copy of both nuclei following mitosis (Alexopoulos and Mims 1979). The classical view of the dolipore is that, whilst it prevents random migration of nuclei and mixing of organelles, it maintains cytoplasmic continuity between adjacent cells so that transport of molecules can occur along the hyphae in the symplast. The extent to which the septum is a barrier to this depends on the size of the pore, viscosity of its content and whether any occlusions are present, as for any symplastic connection (Gunning and Robards 1976, Gunning and Overall 1983, Robards and Lucas 1990).

The structure of the dolipore septum in basidiomycetes has been extensively studied, but mostly from a taxonomic viewpoint and using conventional methods of fixation and embedding (Moore 1984, Lü and McLaughlin 1991). Unfortunately, methods which use chemical fixatives in aqueous solutions produce a number of artefacts. These include characteristic swelling of the septal wall at the rim around the pore, changes in dimensions of the pore, loss of filamentous structures and changes in the structure and relationships of membranes (e.g., Hoch and Howard 1980, 1981; Howard and O'Donnell 1987). These artefacts make it difficult to draw useful conclusions about the structure and transport capacity of the dolipore. Freeze-substitution avoids many of the artefacts and preserves structures which are not usually found after chemical fixation (Howard and O'Donnell 1987, Lingle 1989), and a large amount of work illustrates the value of this technique in preserving fungal ultrastructure. This is especially

* Correspondence and reprints (present address): School of Botany, The University of Melbourne, Parkville, Vic. 3052, Australia.

important for relationships of membranous structures, the size and shape of compartments or pores, and elements of the cytoskeleton. Hoch and Howard (1980, 1981) were the first to examine septal structure in freeze-substituted hyphae of basidiomycetes. Their work with the holobasidiomycete *Laetisaria arvalis* Burds. showed that septal swelling after freeze-substitution was only about one third of that after chemical fixation. A recent paper on septal structure in the heterobasidiomycete *Auricularia auricula-judae* (Bull.: Fr.) Schroet., also using freeze-substitution, revealed new cytoplasmic features of relevance to the maintenance of the dolipore septum and its role in transport (Lü and McLaughlin 1991).

We have examined the development of the dolipore septum between the tip and penultimate cell, and also the structure of mature, apparently functional, septa in *Pisolithus tinctorius* (Pers.) Coker & Couch. Strains of this species form ectomycorrhizas with many forest tree species and the structure of septal pores is relevant to longitudinal transport of nutrients along hyphae from the soil to the tree root system. The hyphal tips of *P. tinctorius* contain a highly motile pleiomorphic vacuole and tubule system which accumulates the fluorochrome 6-carboxyfluorescein. Tubules of this system transport fluorochrome between vacuole clusters situated at intervals along the apical and penultimate cells (Shepherd et al. 1993 a) and across the dolipore septum (Shepherd et al. 1993 b). This transfer is very active during and just shortly after the completion of the dolipore complex between the apical and penultimate cells. We have examined dolipore structure and development in these septa precisely at this stage in freeze-substituted hyphae.

Materials and methods

Pisolithus tinctorius, isolate DI-15 (Grenville et al. 1986), was grown at 21 °C in the dark on modified Melin Norkrans agar medium (Marx 1969), with the following variations: 1.0% agar, 1.0% D-glucose instead of sucrose, light dried malt extract instead of paste, and 3.0 ml/l of 1.0% ferric citrate instead of $FeCl_3$. Hyphae were grown over 5 mm diameter discs of autoclaved cellulose nitrate/acetate filters (Nuclepore brand 'Membrafil' gridded membrane filter, 8.0 µm pore size) placed on the agar surface ahead of the growing hyphal front. Five samples of mycelium from the growing edge of each of 5 culture plates were cut from the agar and frozen on a copper block which was cooled in a bath of liquid nitrogen. They were then freeze-substituted in 2% OsO_4 in acetone at − 70 °C for 6 d, and embedded in Spurr's resin (Spurr 1969) as described in Shepherd et al. (1993 a). Each of these 25 pieces (5 × 5 replicates) of flat-embedded mycelium were subdivided into 1 × 1 mm pieces and examined by light microscopy to select either young or older cells which did not show evidence of ice crystal damage. Sections were cut and stained for 10 min in 2% uranyl acetate in methanol and 20 min in undiluted lead citrate (Reynolds 1963). Some hyphae were freeze-substituted in 20% acrolein in diethyl ether for 32 d, embedded in Spurr's resin, and ultrathin sections were triple stained (Daddow 1983). Electron micrographs were taken with an Hitachi H-7000 transmission electron microscope at 100 kV. Averages of measurements made from electron micrographs are cited as means ± 95% confidence limits (sample size given in brackets). At least ten mature septa and three developing septa were examined. Many were serially sectioned.

For scanning electron microscopy, samples were fixed in 2.5% glutaraldehyde in 0.025 mol/l potassium phosphate buffer, dehydrated in an ethanol series, transferred to 100% acetone and critical point dried. They were sputter coated with gold/palladium and examined in a Cambridge S-360 scanning electron microscope with an accelerating voltage of 20 kV.

Results

Clamp connections and dolipore septa

The formation of the dolipore septum in *P. tinctorius* follows the pattern typical for basidiomycete fungi. As the hypha grows it periodically forms septa which separate the apical cell from the penultimate cell. The septa form just after the two nuclei have undergone mitosis. One nucleus divides in the plane parallel to the longitudinal axis of the hypha and a septum forms perpendicular to this between the two daughter nuclei. Concurrently the second nucleus divides in an oblique plane and one of its progeny moves into the clamp connection, a short anabranch that is initiated anterior to the site of the main septum. Formation of the clamp's septum temporarily isolates this nucleus in the clamp. The clamp cell then fuses with the subterminal segment re-establishing the dikaryon. Two septa are therefore formed: one in the clamp and the other across the main hypha. If branching occurs, the new penultimate cell produces the branch on the basal side of the main septum, and a second clamp forms when this branched penultimate cell divides to cut off a tip cell (Figs. 1 and 2).

Early development of the dolipore septum

In these hyphae of *P. tinctorius* we found that development of the septa in the clamp and main hypha was synchronised (Fig. 3). Each septum was formed by invagination of the plasma membrane perpendicular to the long axis of the cell, with concurrent wall deposition (Figs. 3–7). The septal wall material was similar in appearance to the lateral hyphal wall and was confluent with it (Figs. 3 and 4). At this stage the septum was centripetally tapered. The plasma membrane was closely appressed to the new wall and appeared more electron-opaque than elsewhere. At the inner edge of

the ingrowing septum, the membrane was less clearly defined and its trilaminar structure was not apparent. The cytoplasm in this region appeared more electron-opaque than elsewhere (Figs. 3 and 4) and contained fine filaments (Figs. 3–7). A group of filaments, situated just internal to the centripetally expanding membrane, was in transverse profile in median sections of the ingrowing septum (Fig. 4), while filaments were in longitudinal profile in non-median sections passing through the edge of the pore (Figs. 3, 5, and 7). The latter extended across the pore and some continued as far as the lateral walls of the parent hypha (Fig. 5). Serial sections showed that many of these filaments formed a ring just inside the invaginating membrane. Clusters of filaments in transverse section often occurred at the junction of the septal and lateral walls (Figs. 3 and 6).

Small vesicles were common in the cytoplasm along the sides of the newly developing septum, interspersed amongst the filaments (Figs. 3 and 7). These vesicles were surrounded by a unit membrane (Fig. 7) and had a moderately electron-opaque content. They were circular in profile and were shown in serial sections to be small spherical organelles rather than tubules. Multivesicular bodies and mitochondrial profiles were also frequently seen in the vicinity of the septum. The mitochondria, which were long and cylindrical, tended to span the incipient pore region (Fig. 3). Smooth membrane cisternae also frequently spanned this region at this stage. The multivesicular bodies were circular or elongate in profile and contained small vesicles which were usually more or less spherical (Fig. 8). These internal vesicles were complex, with a centre of low electron-opacity surrounded by a more electron-opaque region with a fuzzy coat. Most were similar in size (34 ± 2 nm, $n = 30$) but some larger ones were occasionally seen (Fig. 8). Rough ER was common adjacent to the developing septum and occasionally was also found parallel to the longitudinal wall of the main hypha. Broad flat profiles of a membrane-enclosed compartment with finger-like projections and sometimes connected with smooth tubular cisternae were commonly found around the invaginated membrane apex (Figs. 9 and 10). An elongate vacuole, of a similar diameter to those seen interconnecting groups of vacuoles in other hyphae, was observed in the vicinity of the developing septum in one instance.

At a later stage of development where the pore was now much narrower the clamp tip had not yet fused with, or dissolved, the lateral wall of the main hypha and the nucleus was still within the clamp (Fig. 11). The septum in the main hypha was at a similar stage of development to the clamp septum. Serial sections through the latter showed that the septal pore apparatus had not yet developed (Figs. 12–16). Electron-opaque material was seen on either side of the septum at the mid-point but no structural detail could be discerned (Fig. 12). The orifice of the pore was more electron-opaque than the surrounding cytoplasm (Figs. 13 and 14). A mitochondrion was continuous through the pore (Fig. 14). Tubular cisternae occurred in the vicinity of the septum (Fig. 12) and could be traced along adjacent to the septum (Figs. 14 and 15), but there was no parenthesome or rough ER characteristic of mature septa. In Fig. 15 the septum was again continuous, indicating that only two sections in the series cut through the pore. There was electron-opaque material in the cytoplasm at the mid-point of the septum (Fig. 15), as there was on the other side of the pore. In the final section of the series (Fig. 16) this electron-opaque material was not present.

The pore complex of mature septa

The pore was barrel-shaped with a diameter of about 76 nm ($n = 10$) at the entrance and 120 nm ($n = 10$) at the midpoint of the wall (Figs. 17–20), and was surrounded by the dolipore which was about 265 nm ($n = 3$) thick in median sections. On either side was a perforated parenthesome characteristic of holobasidiomycetes. The parenthesome appeared as a cisterna-like structure apparently bounded by a unit membrane and with a content of alternating electron-opaque and electron-lucent layers in a very complex pattern (Figs. 17–

Fig. 1. Scanning electron micrograph of a chemically fixed hypha showing a branch point with two clamp connections (*C*). Arrows indicate the direction of growth of the clamps. The predicted positions of the septa in the main axis (S_1) and its clamp connection (S_2), and of the branch (S_3) and its clamp (S_4) are indicated

Fig. 2. Transmission electron micrograph of a freeze-substituted hypha sectioned in a similar orientation to that in Fig. 1 to show the actual positions of the septa labelled S_1–S_4. Three (S_1, S_3, and S_4) are sectioned more or less in the median plane showing mature dolipores and their parenthesomes (*P*). Vacuoles (*V*) are prominent in all three cells. Cisternae of rough ER lie alongside and parallel to each septum and extend for some distance along the longitudinal wall in some cases. The surface of the hypha has an irregular coating of fibrillar material (*EC*) radiating from its surface; this is common in freeze-substituted material but is mostly removed during conventional specimen preparation

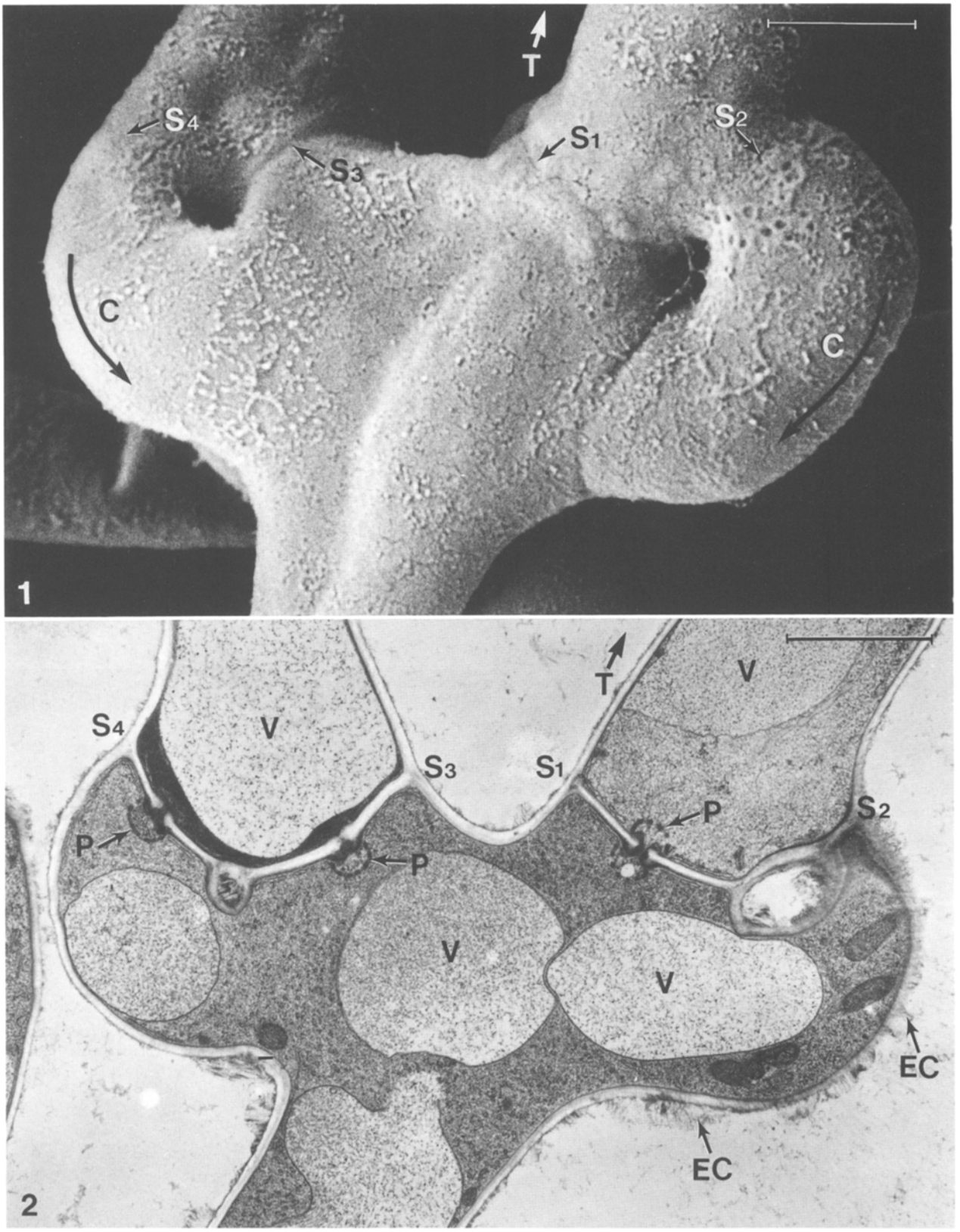

Figs. 1 and **2.** Branched hyphae showing two clamp connections. The direction of the hyphal tip is indicated by the arrow labelled *T* in each case. Bars: 2.0 μm

19). The thickness of the parenthesome, i.e. the distance between the two outer surfaces (43 ± 2 nm, n = 14), was slightly greater than the thickness of the rough ER. The rim of the parenthesome was located very close to the plasma membrane with a more or less perpendicular orientation, often with electron-opaque material bridging the gap. On the plasma membrane and more or less in line with the edge of the rim of each parenthesome there was a series of small electron-opaque deposits (Figs. 17–19). In the best preserved material, these were approximately aligned with the inner and outer membrane and central region of the parenthesome (Figs. 18 and 20). In the ether/acrolein freeze-substituted material, where some material had evidently been extracted, there were small filaments radiating from these deposits for a short distance towards the parenthesome. In one area, where the fine layer of electron-opaque material had pulled away from the plasma membrane, a fine filament connected an electron-opaque deposit within this layer to the parenthesome (Fig. 20).

A single rough ER cisterna profile occurred on each side of the parenthesome on either side of the septum parallel to the septal wall. It was obvious in acetone/osmium freeze-substituted material (Figs. 17–19), but not ether/acrolein freeze-substituted material (Fig. 20), although very close scrutiny of Fig. 20 shows electron-lucent areas where it may have been. Lumen continuity could not be demonstrated between the parenthesome and any of these rough ER profiles, although the two often lay very close together and electron-opaque material appeared in some instances to bridge the gap between them (e.g., Fig. 18). Ribosomes were sparse and were only seen on the cytoplasmic side of the rough ER (Fig. 19). Small filaments connected the septal side of the rough ER to the plasma membrane (Figs. 18 and 19).

Electron-opaque material was usually found in the lumen of the septal pore, often filling it and extending to spread across the pore entrance and the surrounding septal pore swelling (Figs. 17–19). This material varied in appearance according to the freeze-substitution technique used (compare Fig. 18 with 20). It often contained fine filaments and showed distinct electron-opaque bands with an orientation perpendicular to the pore channel. Filaments parallel to the pore channel connected with the transverse bands. The material which spilled out of the pore entrance and over the adjacent

---

Fig. 3. The two septa are laid down more or less synchronously after the clamp has formed and the nucleus (*n*) has migrated into it, but before its tip has fused with the penultimate cell. No septal pore apparatus is present at this stage and there are no rough ER cisternae lying alongside the septum. The septum across the main hypha (S_1) is in tangential section at the edge of the pore, while that across the base of the clamp (S_2) is more or less median. Profiles of mitochondria (*m*) and multivesicular bodies (*mvb*) are abundant and there are short ER cisternal profiles through the area. Microtubules (*mt*) near the septum (S_1) are in various orientations. Filaments (*f*) in longitudinal profile occur in a band across the pore of S_1, while clusters of filaments (*f*) in transverse section occur adjacent to the innermost part of the invaginating membrane in S_2. Small circular profiles of microvesicles (*mv*) with electron-opaque contents are common

Fig. 4. Another septum sectioned close to the median plane shows the transversely sectioned filament (*f*) clusters in greater detail. A membranous reticulum (*r*) is present at the apex of the invaginated septal membrane and microvesicles (*mv*) also occur in the vicinity. Profiles of mitochondria (*m*) and multivesicular bodies (*mvb*) can also be seen

Fig. 5. Tangential view of a septum, more or less at the edge of the pore. The filaments (*f*) are now mostly in longitudinal profile. They extend across the pore and along the flanks of the newly developed septum, showing a more complex pattern around the apex of the infurrowing membrane. The membrane becomes indistinct at its innermost point and in one area (arrowheads) there appears to be a semicircle of fine filaments radiating from it at its tip

Fig. 6. Section showing the complexity of arrangement of fine filaments around the edge of the septum (arrowheads). Two filaments, partly beaded structures, follow the contour of the membrane in a concentric pattern, while radiating spokes perpendicular to the membrane pass across these. One of these spokes passes through a circular profile of electron-opaque material, and there are other circular profiles following the same concentric pattern

Fig. 7. Section showing electron-opaque microvesicles on both sides of the developing septum. One of these (*mv*) is delimited by a distinct unit membrane

Fig. 8. Multivesicular bodies (*mvb*) in the vicinity of the septum are delimited by a characteristic unit membrane with a central electron-lucent region flanked on either side by a layer of electron-opaque material. The internal 'vesicles' do not show this, but appear to be bounded by a single electron-opaque layer which commonly has short electron-opaque 'spokes' radiating from it

Fig. 9. Dilated sheet-like membranous cisternae extend finger-like processes around the apex of the extending membrane of the septum (arrowheads)

Fig. 10. Similar membrane-enclosed sheets (arrowheads) occur around the membrane apex and link up with smooth tubular cisternae (*t*) which extend away from the septum

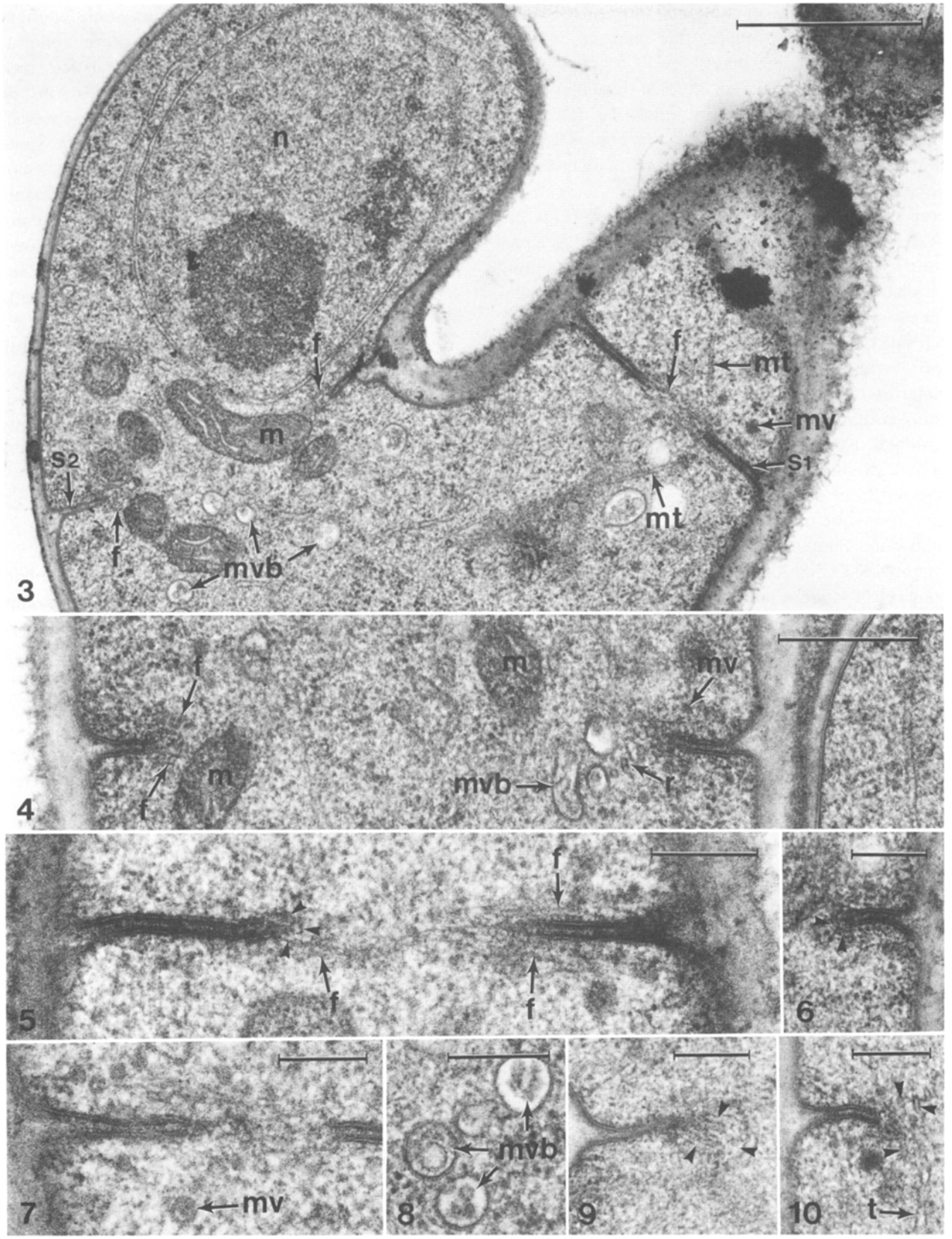

Figs. 3–10. Transmission electron micrographs from two sets of serial sections of freeze-substituted hyphae cut longitudinally through the clamp connection to show early stages of development of the two septa. Bars: Fig. 3, 1 μm; Fig. 4, 0.5 μm; Figs. 5–10, 0.25 μm

septal pore swelling also contained filaments (Figs. 17 and 18) and in several places fine filaments radiated from it to the parenthesome (Figs. 17, 18, and 20). In Fig. 20 at the pore orifice on one side the material had contracted away from the wall indicating that it had cohesiveness. At the other side it was connected with the electron-opaque layer from which a filament radiated to the rim of the parenthesome.

Serial sections through the dolipore septum (Figs. 21–26) showed that rough ER cisternae occurred as a perforate sheet on either side and parallel to the septum at a distance of 18.3 ± 0.3 nm from the plasma membrane (n = 10). The parenthesome formed a dome over each side of the dolipore and was perforated with regularly arranged hexagonal pores with an average diameter of 75 nm (n = 27) (Figs. 22 and 23). Regularly arranged filaments 10 ± 2 nm wide (n = 7) were seen to radiate from the electron-opaque material around the pore swelling to the parenthesome with which they appeared to be confluent (Figs. 24 and 25). Again the electron-opaque material was continuous through the septal pore. Some of the filaments were narrow and straight-sided (Fig. 25) while others appeared coated with electron-opaque material (Fig. 24). The parenthesome rim was very close to the plasma membrane in several places. It appeared confluent with it in tangential view (Fig. 22) and appeared to be attached to it via electron-opaque deposits in median section (Fig. 26). There was also a very close spatial relationship between the parenthesome and rough ER (notably in Figs. 22, 23, and 26), but in no instance could the membranes or lumen be demonstrated as continuous.

In sections cut approximately parallel to the septum (Figs. 27–32), the hexagonal pores of the parenthesome were seen to be arranged in a 'honeycomb' configuration. There were three concentric rows containing 1, 6, and 12 pores respectively. Again, filaments were seen in some sections, radiating from what appeared to be a ring of electron-opaque material surrounding the septal pore, to contact the parenthesome (Fig. 31). Some of the filaments appeared as a continuous series of arrowhead-like structures (Fig. 31). These filaments were present in most sections (Figs. 28–31), but are sectioned at various angles and not always obvious. The electron-opaque material around the pore contained a complex network of interconnected filaments (Figs. 30 and 31) and filamentous structures were found in the entrance to the pore itself (Fig. 31). Presumably these were the longitudinal filaments sectioned obliquely as they radiate out from the pore entrance. There was therefore a very complex pattern of filaments in the sub-parenthesome area.

Discussion

General considerations

The two septa in the main hypha and clamp are laid down synchronously over a matter of minutes. This was demonstrated by Orlovich and Ashford (1993) using differential interference contrast microscopy of live cells. In fig. 3 of their paper there is no septum across the main hypha, while in their fig. 4, taken 5 min later, the septum is complete. The fixed image of this septum (Orlovich and Ashford 1993: fig. 6) shows a dilated structure associated with septum which is interpreted as a dolipore. A similar very rapid rate of septum formation (i.e., completed within 4 min) is reported in *Auricularia auricula-judae* by Lü and McLaughlin

Fig. 11. Although the septum is almost complete, the clamp, which contains a nucleus (*n*), has not yet fused with the main hypha. Mitochondrial profiles (*m*) occur on both sides of the narrowing pore and are connected by a narrow thread (arrowhead) across the pore. The small size of the pore is indicated in Figs. 12–16, which are consecutive sections in a series, only two of which pass through the pore. None of these sections show the parenthesome typical of mature dolipore septa. A tubular cisterna is detected lying alongside the septum in two of the sections. Bar: 1.0 µm

Fig. 12. Section adjacent to the pore. Note the electron-opaque material (arrowheads) on either side of the septum more or less at its midpoint and the tubular cisternae (*tc*) near the septum

Fig. 13. Section through the pore shows electron-opaque material (arrowheads) in the pore and spreading on either side. There is no evidence of microtubules or microfilamentous bundles running longitudinally through the pore. There is no parenthesome and no septal pore swelling

Fig. 14. An enlargement of Fig. 11 showing the bridge through the pore (arrowheads) connecting the mitochondrial profiles (*m*) on either side of the septum. The pore is 140 nm wide. A tubular cisterna (*tc*) is present near the junction of the septum with the longitudinal wall

Fig. 15. The next section again shows the septum as continuous wall, indicating that the outer edge of the pore has been reached. Electron-opaque material (arrowheads) spreads across the wall on either side of the septum close to its mid-point. The tubular cisterna (*tc*) may again be detected and appears continuous for some distance along the septum

Fig. 16. The next section also shows continuous wall but with little electron-opaque material adjacent to it

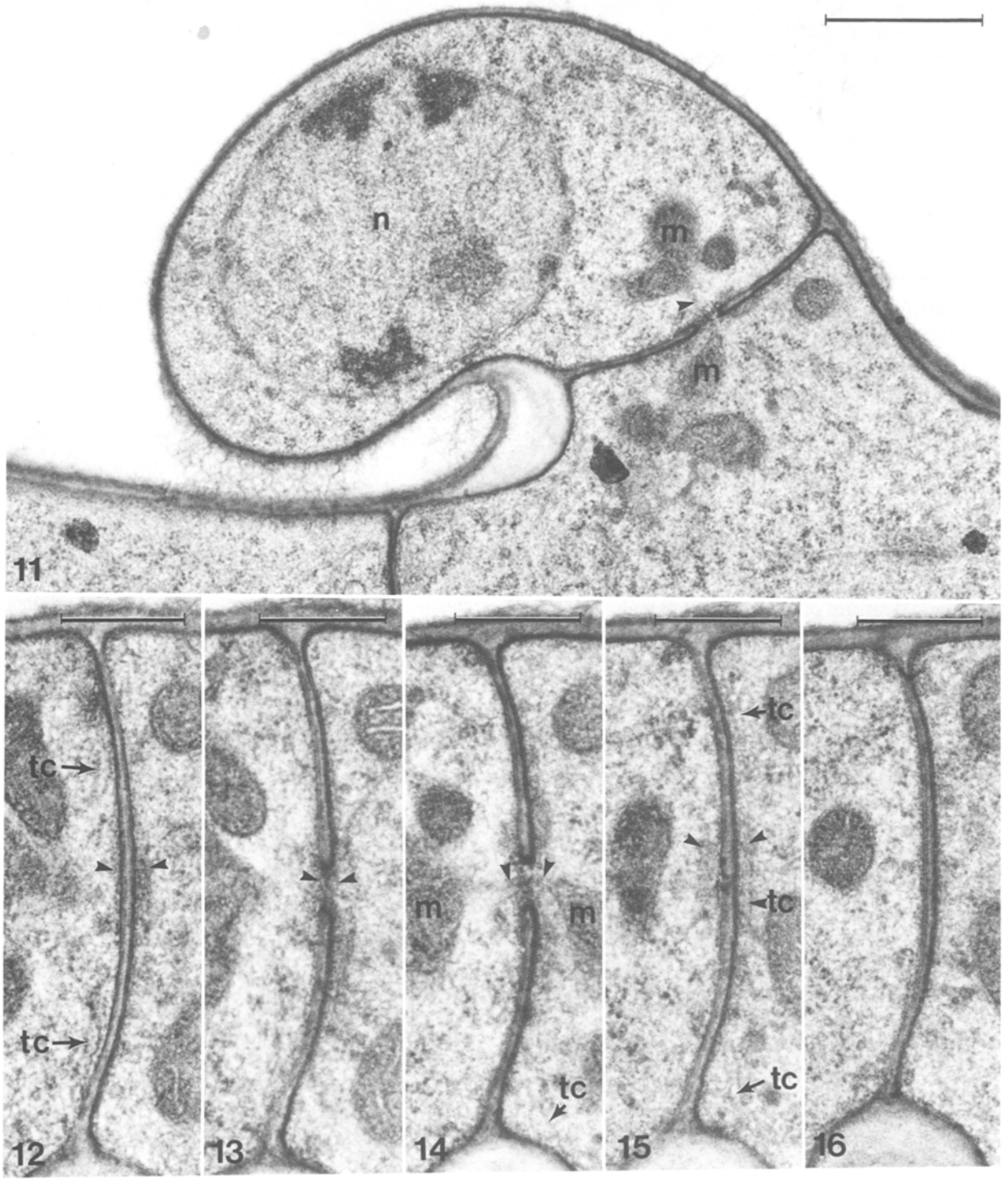

Figs. 11–16. Serial sections through a septum of a freeze-substituted hypha late in development when the pore is almost complete. Bars: 0.5 μm except Fig. 11

(1991). Septum formation involves invagination of the plasma membrane and appears basically similar to cleavage in animal cells (Beams and Kessel 1976), except that the furrowing membrane concurrently secretes cell wall material and this presumably further stabilises the structure. This has also been reported for other higher fungi and contrasts with cytokinesis in higher plant cells, where the cell wall is deposited as a cell plate which extends out centrifugally to fuse with the parent cell wall in a predetermined region of the cell cortex (Gunning 1982). In animal cells, the cleavage furrow forms precisely in the plane of the metaphase plate at right angles to the long axis of the mitotic spindle. Its position is controlled midway between the two asters originating from the two centrosomes and it frequently traps longitudinal arrays of microtubules as cytokinesis progresses (Beams and Kessel 1976). A spatial relationship between nuclear division and cytokinesis has been reported in fungi (see Girbardt 1979) and may also be the case in *P. tinctorius*, but there are very few microtubules left in the region as the septum forms.

Several general features of septal development, such as the occurrence of fine filaments adjacent to the developing septum, membrane invagination and microvesicles in the vicinity, are reported from chemically-fixed as well as freeze-substituted septa in a number of other fungi. However, freeze-substitution also reveals new features in *P. tinctorius*, some of which have been shown only recently in freeze-substituted septa of the heterobasidiomycetes *Tremella globospora* Reid and *Auricularia auricula-judae* (Berbee and Wells 1988, Lü and McLaughlin 1992).

Membrane furrowing and the filamentous ring

Septa form by invagination of the plasma membrane. Although controversial (see Wessels 1986), in growing hyphal tips it seems most likely that the protoplast exerts a positive pressure on the wall to create the necessary expansion at the tip, that is the apex is under turgor pressure. Under these conditions formation of a cleavage furrow is only possible if the plasma membrane is physically pulled inwards by some cytoskeletal element. The plasma membrane of the developing septum is in close association with filaments some of which are oriented in a ring around the circumference of the narrowing pore. A similar structure, sometimes called a filamentous septal belt, has been shown to be associated with septum formation in a number of other

Fig. 17. Median section through a pore. The septum (*s*) is swollen around the septal pore. The plasma membrane (*pm*) is continuous through the septal pore, which contains electron-opaque material. This material spreads out on either side over the septal pore swelling. The diameter of the pore at its mid-point is 106 nm while at the entrance the pore diameter is only 44 nm. Rough ER (*er*) with occasional ribosomes lies parallel to the septum and is not continuous with the parenthesome (*p*) in this section. The parenthesome shows concentric fine bands of electron-opaque material alternate with areas of lower electron-opacity and it is assumed that this parenthesome is sectioned just at the edge of several pores. At one of its ends, the parenthesome is rounded (arrow) and appears to have fine threads radiating from it. There are small electron-opaque deposits on the plasma membrane opposite to the end of the parenthesome on each side of the pore; these are most clear in the regions labelled with arrowheads. In some parts, the septal wall swelling has a 'bubbled' appearance at its edge (double arrow), which may be an artefact where the wall has retracted away from the outer leaflet of the plasma membrane

Fig. 18. The parenthesome contains alternating electron-opaque and electron-lucent bands, the outermost group of which is presumed to be the limiting unit membrane. These bands are occasionally spanned by transverse filaments (*tf*). The parenthesome surface carries an irregular deposit of electron-opaque material; this is most obvious on the septal side, where occasionally it extends into fine radiating strands of electron-opaque material (*st*). At one end (double arrow) the parenthesome is rounded. Small electron-opaque deposits (arrowheads) on the plasma membrane are again found opposite to the ends of the parenthesome, and fine filaments appear to attach the parenthesome ends to these deposits (e.g., arrow). Other filaments (*f*) radiate from the parenthesome at the edge of one of its pores. Several transverse electron-opaque bands (*b*) are seen in the septal pore. Fine filaments run across these longitudinally through the pore

Fig. 19. This section passes obliquely through the septal pore. Ribosomes (*r*) on the rough ER parallel to the septum are present only on the cytoplasmic side. Small filaments connecting the plasma membrane to the rough ER can just be detected (arrowheads). There are also fine, sometimes beaded filaments (arrows) radiating from the region adjacent to the pore mouth towards the parenthesome

Fig. 20. In this section of ether/acrolein freeze-substituted material, five distinct electron-opaque bands (*b*) are seen in the septal pore. Some of these are beaded. Again the pore filling material contains longitudinal filaments and these terminate at cross bands. Electron-opaque deposits occur on the plasma membrane adjacent to the ends of the parenthesome and some of these are extended into short filaments (arrowheads). At one point where filamentous electron-opaque pore-filling material (*om*) is spread over the pore swelling, but appears to have been displaced from the plasma membrane, this material is connected to the end of the parenthesome by a single fine strand (*f*). The electron-opaque material (*om*) is continuous across the pore and extends over the plasma membrane on the other side along the septum. There is an electron-lucent layer around the edge of the septum across which there are also very fine transverse filaments. The septal pore swelling is mostly electron-opaque, with an electron-lucent longitudinal band in the mid-point of the wall

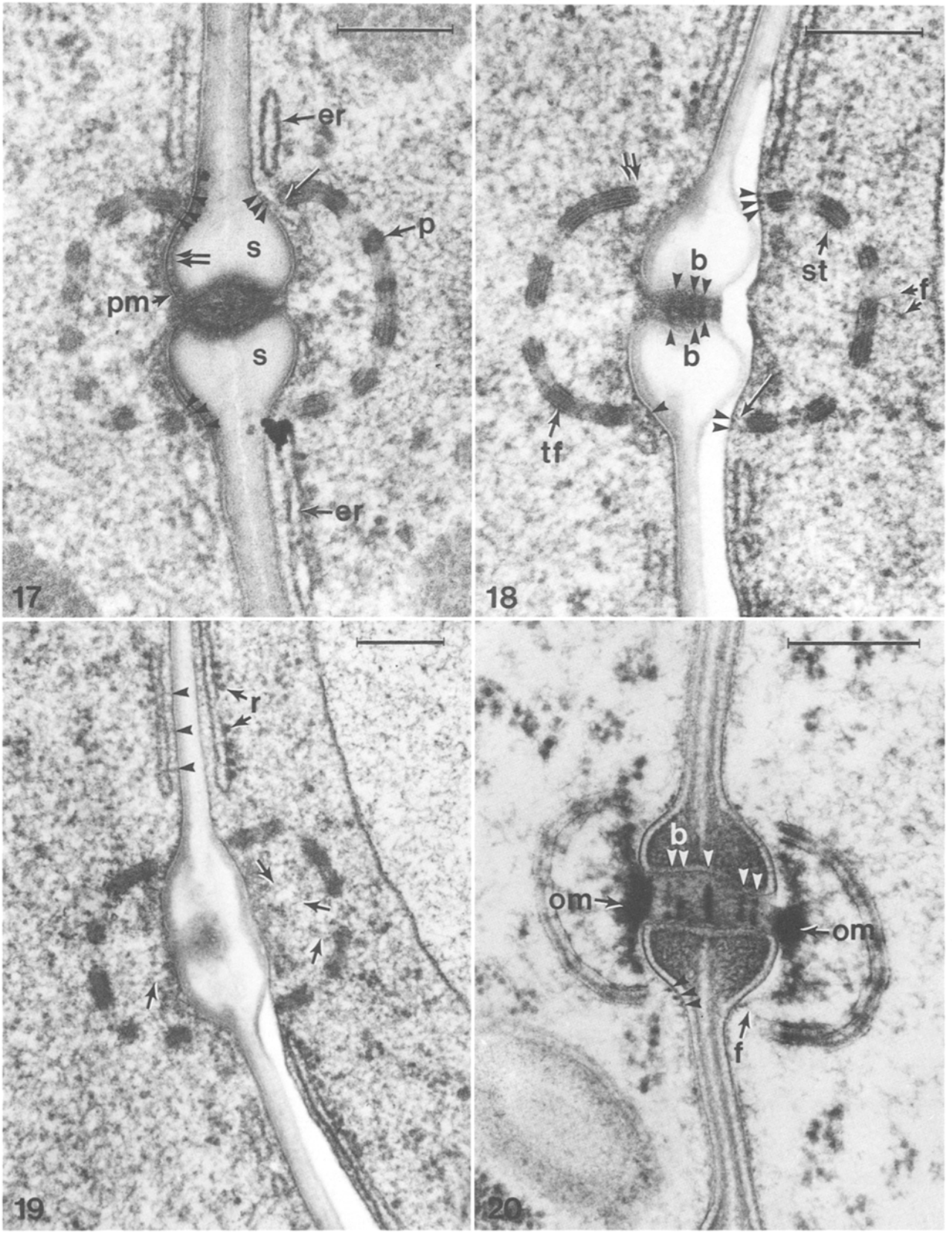

Figs. 17–20. Ultrastructure of fully-developed dolipore septa freeze-substituted in either 2% OsO_4 in acetone (Figs. 17–19) or 20% acrolein in diethyl ether (Fig. 20). Bars: 0.25 μm

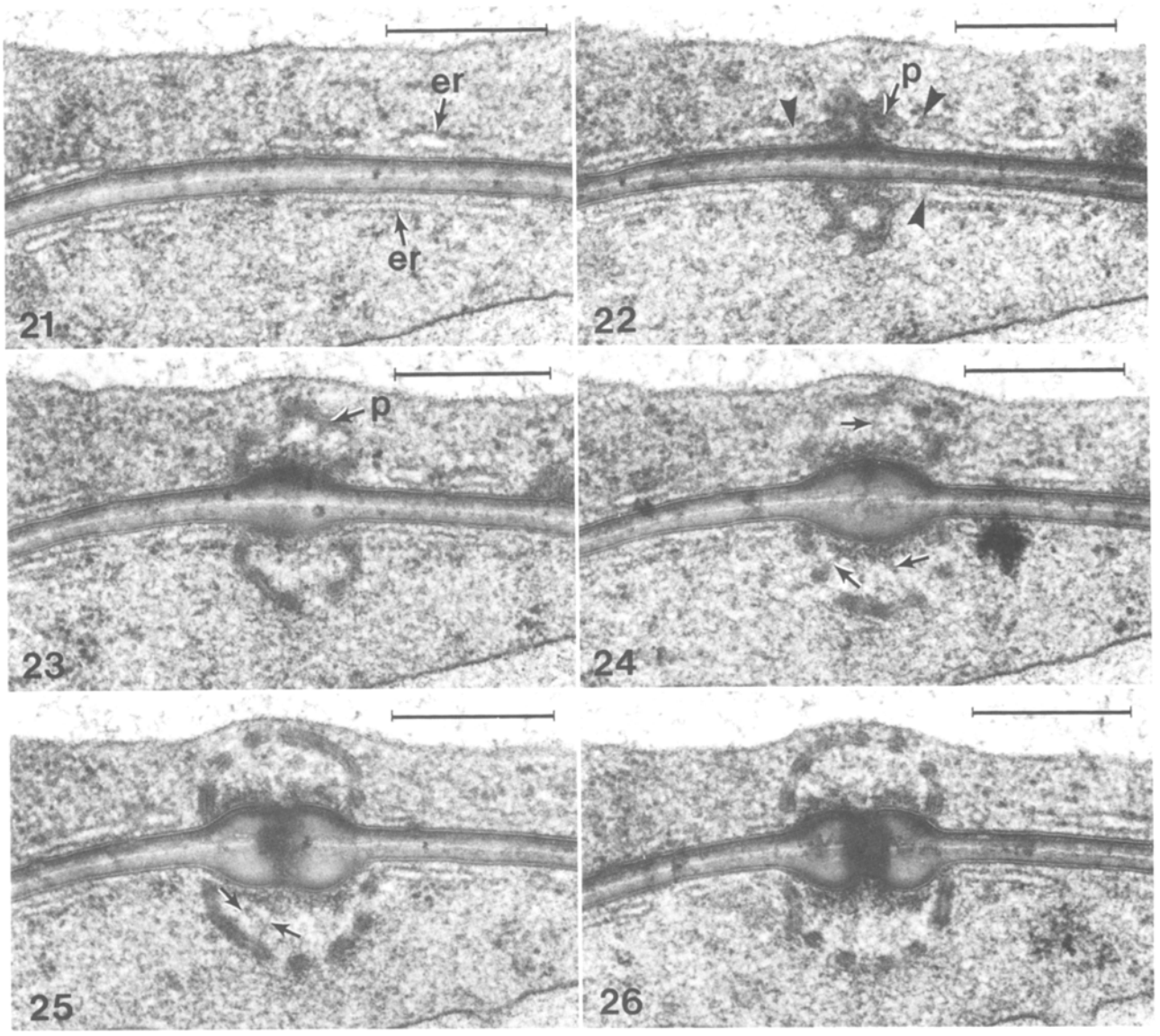

Figs. 21–26. Serial sections through a freeze-substituted dolipore septum cut approximately perpendicular to the septum. Bars: 0.5 μm

Fig. 21. The first section misses the dolipore and shows a septal wall with no gap, bounded by a plasma membrane. Lying on both sides of the septum and parallel to it is rough ER (*er*). This is discontinuous and is seen in subsequent sections (Figs. 22–26), indicating that it occurs as perforated sheets

Fig. 22. The edge of the parenthesome (*p*) is in this section. It extends to contact the plasma membrane on both sides of the septum. Rough ER is very close to the parenthesome at several points (arrowheads) but no lumen continuity is apparent. On the upper side of the septum, the beginnings of the septal pore swelling are apparent. Several perforations, one of which is hexagonal in profile, can be identified in the parenthesome of the lower cell

Fig. 23. The septal pore swelling is now apparent on both sides of the septum. In the upper cell the electron-opaque material can be seen between the parenthesome and the membrane-wall interface. Perforations are seen in the parenthesome (*p*) of the upper cell

Fig. 24. The septal pore swelling now appears larger and electron-opaque material lies in a layer on either side of it beneath the parenthesome; it is spread out to cover the entire area below the parenthesome dome. Fine filaments (arrows) radiate from this electron-opaque material to the parenthesome

Fig. 25. At least two filaments (arrows) radiate between the parenthesome and the septum in the lower cell. They are embedded in electron-opaque material and one radiates from the edge of the pore entrance

Fig. 26. Median section shows that the electron-opaque material is continuous through the central pore

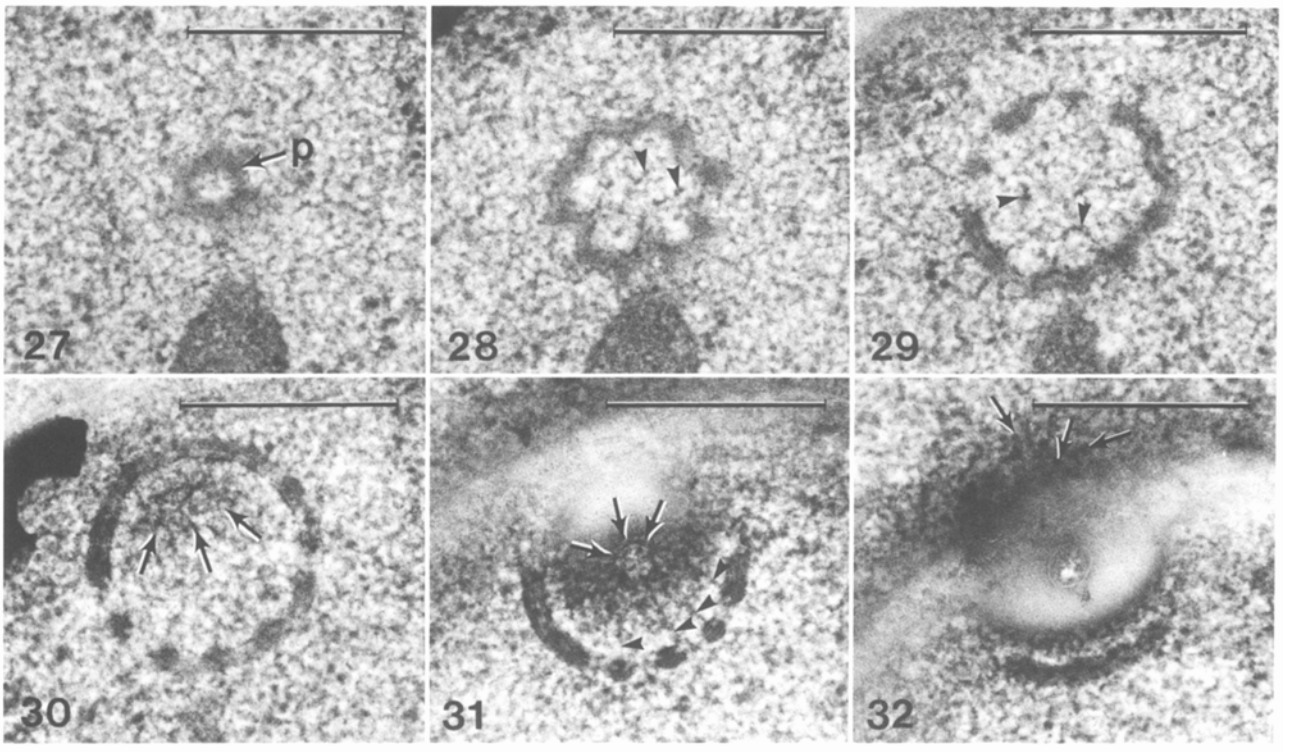

Figs. 27–32. Serial sections through another freeze-substituted dolipore septum, cut approximately parallel to the septum. Bars: 0.5 µm

Fig. 27. The first section shows the top of a parenthesome (*p*) surrounded by cytoplasm. There is a single perforation

Fig. 28. The adjacent section cut below shows that the single perforation is surrounded by a second layer of six perforations. Electron-opaque dots in the sub-parenthesome cytoplasm (arrowheads) are interpreted to be filaments sectioned at various angles

Fig. 29. In the next section a third layer of perforations is seen. Electron-opaque dots (arrowheads) are again present in the sub-parenthesome cytoplasm

Fig. 30. This section just grazes into the sub-parenthesome cytoplasm situated just above the pore, showing electron-opaque filaments radiating from the parenthesome membrane to a mass of electron-opaque material (arrowed region) containing a network of fine filaments

Fig. 31. The section (cut below Fig. 30) shows several filaments (arrowheads). All radiate from what appears to be an inner electron-opaque mass towards the parenthesome. Most contact the parenthesome and in one case the direct contact is seen to be with the electron-opaque material overlying the membrane

Fig. 32. The final section passes through the septal pore which is partially occluded by electron-opaque material. A number of electron-opaque circular profiles (arrows) are seen embedded in this material, overlying the septal pore swelling

fungi (e.g., Patton and Marchant 1978, Girbardt 1979, Hoch and Howard 1980, Roberson 1992). The ring of filaments in *P. tinctorius* may be a similar structure. This septal belt has been compared with the contractile ring in animal cells, found beneath the furrowing membrane and known to be composed of circumferentially oriented microfilaments associated with other cytoskeletal elements (Rappaport 1986). Actin has been demonstrated at the site of developing septa in the ascomycete *Sclerotium rolfsii* Sacc. and other fungi (see Roberson 1992), and cytochalasin E inhibits septum and septal ring formation in bean rust, *Uromyces appendiculatus* (Pers.) Unger, another basidiomycete (Tucker et al. 1986). However, confirmation that the septal belt consists of F-actin awaits labelling at the ultrastructural level.

Any structure which causes membrane furrowing must have good lateral contact with the membrane. This applies to the filamentous electron-opaque material at the apex of the furrowed membrane around the edge of the pore. There appear to be three sets of filaments all perpendicular to each other. Two of these are parallel to the membrane while the third set is perpendicular to it. Those filaments perpendicular to the membrane appear to anchor it and are probably responsible for pulling it inwards, while the set represented by the electron-opaque circular profiles that these pass through could be part of the contractile ring. The third

set are parallel to the membrane and interconnect the other two. Their arrangement and the appearance of the membrane all indicate an interaction with filaments, with the membrane pulled in at this point. The difference between the appearance of the membrane around the rim of the pore and along the flanks of the septa may simply result from the membrane being more fragile at the innermost region, perhaps resulting from a slight delay between membrane assembly and wall deposition. In animal cells net membrane biosynthesis is reported to occur just before cell division and it is believed that extra membrane required during cytokinesis is stored at the cell surface (Alberts et al. 1989). In *P. tinctorius*, finger-like processes commonly seen extending from flattened cisternae around the apex of the furrowing membrane could perhaps supply membrane very rapidly to the developing septum.

The electron microscopy does not shed any light on how the parenthesome forms, but it does show that it appears late in septal development when the pore has become quite narrow. This indicates that structures such as the larger organelles can move across the septum until very late in septal development and, as shown here, organelles can be trapped and constricted by the rapidly narrowing pore. The septal pore swelling, a feature that characterises holobasidiomycetes and advanced heterobasidiomycetes (Hoch and Howard 1981, Lü and McLaughlin 1991), is not present at this stage either. The septal pore swelling at maturity is about 260 nm at its widest point. This agrees with results from other basidiomycetes. For example in *Laetisaria arvalis* the swelling ranged from 220 to 300 nm in freeze-substituted and 760 to 800 nm in chemically fixed material indicating that it is enlarged about three-fold after chemical fixation. In *Auricularia auricula-judae* it is somewhat narrower, 100 to 184 nm, but is still expanded by about a factor of three by chemical fixation.

Structure of the septal pore complex at maturity

The septum with its dolipore is thought to provide symplastic continuity while excluding organelles. It has been shown here, as in other basidiomycetes (see Lü and McLaughlin 1991), that the sub-parenthesome space is largely free of organelles. The only structures found in this area in *P. tinctorius* are the tubular cisternae which pass through the parenthesome pores to the septal pore entrance (Shepherd et al. 1993 b) and occasional circular membrane profiles which may be these tubules in transverse section or small vacuole profiles. This indicates that the parenthesome, even though perforate, is very effective in excluding organelles from this zone, so that the septal pore entrance is not occluded by any of the larger organelles such as mitochondria. It is noteworthy that the diameter of the parenthesome pores is very similar to the diameter of the septal pore entrance. Therefore in this fungus structures allowed through the parenthesome should also be able to enter and pass through the septal pore. However, it might be envisaged that for efficient movement through the pore, any structure passing through the parenthesome pores would need to be oriented towards the septal pore, so that it does not strike the septal wall rather than the pore entrance. The domed shape of the parenthesome, the position of the parenthesome pores and any guiding elements radiating towards these pores and between these and the septal pore orifice, may all play a part in such guidance. In the absence of microtubules in the sub-parenthesome region it would seem likely that the radiating filaments play some role in direction of movement. No attempt was made to identify the filaments seen here in *P. tinctorius* because there is no chemical information on them. Little significance can be ascribed to differences in size and appearance of the various filaments in the sub-parenthesome region since these are modified by staining, which was quite variable after freeze-substitution in osmium/acetone.

The occurrence of rough ER parallel to the septum on either side of the pore has been reported in a range of basidiomycetes (see Moore 1984). This occurs as perforated sheets, apparently connected to the plasma membrane by somewhat broader filaments (Berbee and Wells 1988, Lü and McLaughlin 1991) at a fixed distance from it. The situation was similar in *P. tinctorius*. Continuity between this rough ER adjacent to the septum and the parenthesome has also been reported from both chemically-fixed and freeze-substituted hyphae (see Moore 1984, Lü and McLaughlin 1991). Lumen continuity between the rough ER and the parenthesome of mature septa could not be demonstrated here in *P. tinctorius* despite searching extensively in serial sections. The ER was always very close to the parenthesome, but the edges of the parenthesome were frequently rounded off and invariably pointed towards the plasma membrane to which they appeared anchored via fine filaments. Our conclusion is that in the mature, apparently fully functional septa of non-senescent cells of *P. tinctorius*, lumen continuities are either very rare or absent altogether. This does not, however, exclude a mechanical contact and electron-opaque material frequently bridged the zone between the parenthesome and ER. The parenthesome contained electron-opaque

material which showed a characteristic banding pattern. The structure, origin and function of this material is not clear but it is tempting to speculate that it may play a role in anchoring the parenthesome to the filaments and may be important in maintaining its shape. The orientation of the rough ER sheets parallel and at a fixed distance from the septal plasma membrane indicates that the filaments bridging the two are probably acting as anchor points between ER and membrane.

Transport and communication through the dolipore

The dolipore frequently appears to be filled by electron-opaque material that is continuous through the pore and spreads across the entrance on both sides. This material is heterogeneous, shows dark transverse bands and appears to contain filaments. It also has some measure of cohesion. Similar 'occlusion' of the pores with electron-opaque material with darker transverse bands is described from chemically-fixed (see Moore 1984) and freeze-substituted septa (Lingle 1989, Bourrett and McLaughlin 1986, Lü and McLaughlin 1991). It varies in appearance and position according to species and fixation conditions, but in general it appears much better preserved after freeze-substitution when the fine filaments and more cross bands are apparent. It is difficult to determine a role for this material in transport since neither its viscosity nor permeability are known. No conclusions can be drawn about its role in blocking or controlling the permeability of the channel. It appears to be pushed aside when tubular cisternae pass across the parenthesome pores and enter the mouth of the pore channel (Shepherd et al. 1993 b). This provides circumstantial evidence that the smooth membrane cisternae do pass through the channel and that the material offers some resistance, at least to larger structures.

It has been shown that tubules connected with the vacuole system transfer a fluorochrome across the dolipore septum between adjacent cells (Shepherd et al. 1993 b). This transfer appears to be most active during and shortly after completion of the septum. It is possible that this transfer might occur at a stage when the septum was incomplete and the dolipore had not yet formed. However, the data here provide evidence that this is not so. Commonly, movement of tubules occurs for periods of at least 45 min (Shepherd unpubl. obs.), while the septum takes only about 5 min to form. Septa in the main hypha and clamp are laid down synchronously and it is shown here that both are completed by the time the clamp fuses with the main hypha, prior to migration of the nucleus back into the main hypha. Tubule movements continue back and forth across the septa until well after this stage, when the heterokaryon has been restored (Shepherd et al. 1993 b, Shepherd and Ashford unpubl. obs.).

Apart from the tubules, organelles are generally excluded from the region between the parenthesome and the pore and it is likely that the parenthesome plays a role in keeping the pore free from structures that have the potential to occlude it. At the same time it would appear that the parenthesome is instrumental in controlling the approach of the smooth tubular cisternae towards the septal pore entrance. Under these circumstances the parenthesome should be firmly anchored and its position precisely maintained in relation to the septal pore entrance. This requirement for precise orientation also applies to the spatial relationship between the septal pore entrance and the parenthesome pores. The filaments that occur between the edge of the parenthesome and plasma membrane would be in an ideal position to anchor the parenthesome around the septal pore, while the many filaments that radiate between the pore entrance and the parenthesome membrane at various points could fulfil the function of keeping the parenthesome in its convex configuration, like the spokes of an umbrella. This would maintain both the shape and orientation of the parenthesome and thus maximise control over movement of tubular cisternae towards the pore entrance, from a wide radius across the hypha. The radiating filaments may also be involved in guiding the movement of tubules or cytoplasmic streams towards the pore entrance.

In conclusion, the parenthesome may be seen not only as an occluding, filtering device as envisaged by Lü and McLaughlin (1991), but also as a structure that positively guides elements towards the septal pore. For efficient function it is imperative that the parenthesome maintains its shape and position in relation to the pore. It is proposed that the various filaments radiating from it towards the pore and those attached to the plasma membrane all play a role in this.

Acknowledgments

This work was supported by an Australian Research Council grant to AEA. Part of this work was completed while DAO was in receipt of an Australian Postgraduate Research Award. The authors thank Suzanne Bullock for preparing the plates and Bill Allaway, Suzanne Bullock, and Virginia Shepherd for comments on the manuscript.

References

Alberts B, Bray D, Lewis J, Raff M, Roberts K, Watson JD (1989) Molecular biology of the cell, 2nd edn. Garland, New York

Alexopoulos CJ, Mims CW (1979) Introductory mycology, 3rd edn. Wiley, New York

Beams HW, Kessel RG (1976) Cytokinesis: a comparative study of cytoplasmic division in animal cells. Amer Scientist 64: 279–290

Berbee ML, Wells K (1988) Ultrastructural studies of mitosis and the septal pore apparatus in *Tremella globospora*. Mycologia 80: 479–492

Bourret TM, McLaughlan DJ (1986) Mitosis and septum formation in the basidiomycete *Helicobasidium mompa*. Can J Bot 64: 130–145

Daddow LYM (1983) A double lead stain method for enhancing contrast of ultrathin sections in electron microscopy: a modified multiple staining technique. J Microsc 129: 147–153

Girbardt M (1979) A microfilamentous septal belt (FSB) during induction of cytokinesis in *Trametes versicolor* (L. ex Fr.). Exp Mycol 3: 215–228

Grenville DJ, Peterson RL, Ashford AE (1986) Synthesis in growth pouches of mycorrhizae between *Eucalyptus pilularis* and several strains of *Pisolithus tinctorius*. Aust J Bot 34: 95–102

Gunning BES (1982) The cytokinetic apparatus: its development and spatial regulation. In: Lloyd CW (ed) The cytoskeleton and plant growth and development. Academic Press, London, pp 229–292

– Overall R (1983) Plasmodesmata and cell-to-cell transport in plants. Bioscience 33: 260–265

– Robards AW (1976) Plasmodesmata and symplastic transport. In: Wardlaw IF, Passioura JB (eds) Transport and transfer processes in plants. Academic Press, New York, pp 15–41

Hoch HC, Howard RJ (1981) Conventional chemical fixations induce artifactual swelling of dolipore septa. Exp Mycol 5: 167–172

Howard RJ, O'Donnell KL (1987) Freeze-substitution of fungi for cytological analysis. Exp Mycol 11: 250–269

Lingle WL (1989) Enhanced staining of the basidiomycete *Panellus stypticus* prepared for transmission microscopy by freeze-substitution. Crypt Bot 1: 236–242

Lü H, McLaughlin DJ (1991) Ultrastructure of the septal pore apparatus and early septum initiation in *Auricularia auricula-judae*. Mycologia 83: 322–334

Marx DH (1969) The influence of ectotrophic mycorrhizal fungi on the resistance of pine roots to pathogenic infections. 1. Antagonism of mycorrhizal fungi to root pathogenic fungi and soil bacteria. Phytopathology 59: 153–163

Moore RT (1984) The challenge of the dolipore/parenthesome. In: Moore D, Casselton LA, Wood DA, Frankland JC (eds) Developmental biology of higher fungi. Cambridge University Press, Cambridge, pp 175–212

Orlovich DA, Ashford AE (1993) Polyphosphate granules are an artefact of specimen preparation in the ectomycorrhizal fungus *Pisolithus tinctorius*. Protoplasma 173: 91–102

Patton AM, Marchant R (1978) A mathematical analysis of dolipore/parenthesome structure in basidiomycetes. J Gen Microbiol 109: 335–349

Rappaport R (1986) Establishment of a mechanism of cytokinesis in animal cells. Int Rev Cytol 105: 245–281

Reynolds ES (1963) The use of lead citrate at high pH as an electron-opaque stain in electron microscopy. J Cell Biol 17: 208–210

Robards AW, Lucas WJ (1990) Plasmodesmata. Annu Rev Plant Physiol Mol Biol 41: 369–419

Roberson RW (1992) The actin cytoskeleton in hyphal cells of *Sclerotium rolfsii*. Mycologia 84: 41–51

Shepherd VA, Orlovich DA, Ashford AE (1993 a) A dynamic continuum of pleiomorphic tubules and vacuoles in growing hyphae of a fungus. J Cell Sci 104: 495–507

– – – (1993 b) Cell-to-cell transport via motile tubules in growing hyphae of a fungus. J Cell Sci 105: 1173–1178

Spurr AR (1969) A low-viscosity epoxy resin embedding medium for electron microscopy. J Ultrastruct Res 26: 31–43

Tucker BE, Hoch HC, Staples RC (1986) The involvement of F-actin in *Uromyces* cell differentiation: the effects of cytochalasin E and phalloidin. Protoplasma 135: 88–101

Wessels JGH (1986) Cell wall synthesis in apical hyphal growth. Int Rev Cytol 104: 37–79